https://doi.org/10.5194/egusphere-2025-1589
Preprint. Discussion started: 24 April 2025

The extratropical tropopause - Trace gas perspective on tropopause definition choice

Sophie Bauchinger[1], Andreas Engel[1], Markus Jesswein[1], Timo Keber[1], Harald Bönisch[2], Florian Obersteiner[2], Andreas Zahn[2], Nicolas Emig[3], Peter Hoor[3], Hans-Christoph Lachnitt[3], Franziska Weyland[3], Linda Ort[4], and Tanja J. Schuck[1]

[1]Institute for Atmospheric and Environmental Sciences, Goethe University of Frankfurt, Frankfurt, Germany
[2]Karlsruhe Institute of Technology, Institute of Meteorology and Climate Research, Karlsruhe, Germany
[3]Johannes Gutenberg University of Mainz, Institute for Atmospheric Physics, Mainz, Germany
[4]Atmospheric Chemistry Department, Max Planck Institute for Chemistry, Mainz, Germany

Correspondence: Sophie Bauchinger (bauchinger@iau.uni-frankfurt.de)

Abstract.

Aircraft measurement campaigns such as IAGOS-CARIBIC and HALO missions are invaluable sources of trace gas observations in the extratropical Upper Troposphere and Lower Stratosphere (exUTLS), providing simultaneous measurements of multiple substances. To contextualise these observations, the use of dynamic coordinate systems such as tropopause-relative coordinates is highly beneficial. Different approaches to define the tropopause are commonly used in studies, based on either differences in chemical composition, dynamical parameters, or temperature gradients between the troposphere and stratosphere. We examine how different tropopause definitions influence the climatology and seasonality of trace gas observations. Meteorological parameters used in this analysis are obtained from ERA5 reanalysis data interpolated to the flight tracks. Our findings indicate that the thermal tropopause results in larger variability near the tropopause. Different potential-vorticity thresholds result in vertically displaced distributions but similar seasonal variability around the tropopause. Of these, the 3.5 PVU threshold best represents the transport barrier at the tropopause as indicated by the sharpest cross-tropopause gradient. Tracer-based tropopauses using O_3 or N_2O can be used effectively to differentiate between the troposphere and stratosphere without the use of additional model data. A chemical tropopause tied to a mid-latitude ozone climatology was shown to return a meaningful tropopause-relative coordinate. An investigation of individual flights showed that the tropopauses calculated from model data did not represent small-scale structures well, while the 'in-situ' chemical tropopauses provided more meaningful results. For the calculations of an N_2O-based statistical tropopause, however, the case studies highlighted the importance of carefully setting initial parameters.

1 Introduction

The chemical and radiative properties of the extra-tropical Upper Troposphere and Lower Stratosphere (ExUTLS) are heavily influenced by atmospheric transport and mixing processes. However, in-situ observations in this complex region are rare, leading to significant uncertainties in our understanding of many processes. Reducing these uncertainties, particularly in

https://doi.org/10.5194/egusphere-2025-1589
Preprint. Discussion started: 24 April 2025

stratosphere-troposphere exchange (STE) processes, is crucial for improving our ability to model current and future climate change. The complexity and interconnectedness between emissions and STE can be characterised better through increased understanding of trace gas distributions in the atmosphere and therefore their long-term impacts. Despite growing scientific interest and research in this region over the past few decades, knowledge gaps and uncertainties persist. To address these, long-term analysis of trace gas distributions is essential for evaluating trends, conducting STE studies, and assessing the strength of transport barriers such as the tropopause.

Analysis of long-term phenomena in trace gas distributions depends to some part on our ability to identify dynamically equivalent air masses over long periods of time. As the atmosphere is a highly dynamic system, the location of transport barriers such as the tropopause and the subtropical and polar jet are not fixed. When analysing long-term data sets, comparing measurements using geometric coordinates (altitude, latitude, longitude) thus introduces additional variability. Improvements can be achieved through the use of coordinates representing natural flow pathways in the atmosphere such as potential temperature, especially in combination with equivalent latitude in the stratosphere (Pan et al., 2012). In the UTLS region, however, changes in trace gas gradients at the tropopause can have a significant impact on the comparability of measurements.

Studies of the UTLS therefore benefit from using tropopause-relative coordinates, which can again be expressed in terms of pressure, potential temperature or other parameters. Millán et al. (2024) systematically show the effects of tropopause-relative vertical coordinates for ozone data in a variety of data sets. Coordinates relative to the subtropical jet were also tested, but this approach did not result in a significant improvement in grouping air masses. On the other hand, the study highlighted the benefits obtained by using potential temperature over pressure for UTLS studies of ozone.

Although tropopause-relative coordinates are widely used in UTLS studies, there is no consensus on the “best” coordinate system. The variety of available tropopause definitions and vertical coordinate options makes it challenging to select the most appropriate system for specific questions, especially considering that the advantages and disadvantages of different tropopause definitions depend on the particular research context. The tropopause has historically been defined by the World Meteorological Organisation (WMO) using the temperature lapse rate (WMO, 1957), later definitions based on atmospheric dynamics (Reed, 1955; Tinney et al., 2022; Turhal et al., 2024) or chemical composition (Bethan et al., 1996; Sprung and Zahn, 2010; Prather et al., 2011; Assonov et al., 2013) emerged.

This work will provide an overview of the most commonly used tropopause definitions in exUTLS studies. Measurements of well-mixed and long-lived trace gases in the upper troposphere and lower stratosphere can be used to quantify how well any tropopause definition represents the differences between the two atmospheric layers. We show the differences in homogeneity around the different tropopauses by calculating binned variability and calculating the cross-tropopause gradients. For a holistic discussion of this topic, we look at two perspectives: First, we compare tropopauses on a climatological scale and then look at individual events. For the climatological analysis, we focus on data collected on-board a passenger aircraft during the second

https://doi.org/10.5194/egusphere-2025-1589
Preprint. Discussion started: 24 April 2025

phase of the IAGOS-CARIBIC (**C**ommercial **A**ircraft for **R**egular **I**nvestigation of the atmosphere **B**ased on an **I**nstrument **C**ontainer) project. We use the temporal resolution of the flask samples for all CARIBIC analyses, as measurements of N_2O are not available at higher resolution. We then take a case-study approach to test the climatological results using individual flights of the PHILEAS campaign of the German research aircraft HALO. The trace gas observations are combined with meteorological parameters from ERA5 reanalysis data interpolated onto the flight tracks.

2 Data

In the second phase of the IAGOS-CARIBIC project, 19 instruments were fitted into a strongly modified LD11 airfreight container, which was loaded onto a passenger aircraft. Through a specially designed inlet system, incoming air was distributed to a variety of in-situ measurement devices and a flask sampler (Brenninkmeijer et al., 2007; Petzold et al., 2015). Owing to the instruments onboard the aircraft, simultaneous high resolution (< 10 s) measurements of O_3, CO and many other substances were taken throughout the entire project. Flask sample data was collected using the air sampling device TRAC (Triggered Retrospective Air Collector) (Brenninkmeijer et al., 2007; Schuck et al., 2009), which consists of 14 glass cylinders. In 2010, flask sample collection was expanded with 88 stainless-steel cylinders with the device HIRES (HIgh REsolution Sampler). Samples were taken every 30 to 60 minutes by pressurising the containers to 4.5 bar using metal bellow pumps upon reaching a pressure level of less than 480 mbar. Total sample collection times were 0.5–1.5 min, resulting in a spatial resolution of 7–21 km. After collection, the following constituents of the air samples were measured at laboratories across Europe: greenhouse gases, non-methane hydrocarbons, halocarbons and isotopic composition. The N_2O measurements used here are part of the greenhouse gas data set and were carried out with an HP 6890 gas chromatograph coupled to an electron capture detector. (Schuck et al., 2009, 2012). As part of the whole-air-sampler (WAS) data set, the N_2O data has been made available in Schuck and Obersteiner (2024),

Meteorological parameters for each observation were obtained by interpolating ERA5 reanalysis data onto the flight tracks and time stamps. The reanalysis data used has a temporal resolution of 6 hours, horizontal grid spacing of 1° and 137 vertical levels, which approximately corresponds to a spacing of 500 m (Hersbach et al., 2020). The available variables include potential temperature, potential vorticity, as well as various parameters describing the distance between the flight track and multiple definitions of the tropopause. The distance between flight track and thermal tropopause was derived by matching the model's pressure levels to the measured in-fight pressure, while dynamic tropopauses, PV and equivalent latitude were first interpolated onto isentropes using potential temperature and then interpolated onto the flight track. The time resolution of the model data was chosen to match the 10 s intervals of the merged high resolution CARIBIC data set. Further interpolation of the model data, as well as high resolution trace gas measurements, was carried out to match the WAS data timestamps. For consistency, all data from the CARIBIC project used in this study are on WAS time resolution.

https://doi.org/10.5194/egusphere-2025-1589
Preprint. Discussion started: 24 April 2025

Measurements taken as part of the CARIBIC project make up a unique data set due to the regularity of flights, the large geographical coverage of the northern hemisphere and the simultaneous observations of a multitude of substances and parameters. Particularly of interest for this study is that in mid- and high latitudes, the cruise altitude of commercial aircraft roughly coincides with the location of the tropopause / UTLS region. We therefore limit the data set to latitudes > 30°N, with the added benefit that all tropopause definitions in this comparison are well-defined in this region. For this subset, we find that at least 65% of measurement points are located within 2 km of the tropopause for all definitions.

For the case studies in Section 4.4, we use observations from the PHILEAS campaign in August and September 2023 aboard the research aircraft HALO (Riese et al., 2024). The transfer flights between Germany and Alaska were chosen as they provide significant geographical coverage and the routes taken were not tailored to explore special features in the atmosphere. A large benefit of this data set is the availability of high resolution in-situ trace gas measurements, including N_2O. The measurements of N_2O were carried out using the University of Mainz Airborne Quantum Cascade Laser Spectrometer (UMAQS) with a total uncertainty of 0.13 ppb after calibration and comparison to NOAA working standards (Müller, 2015). Measurement data from the PHILEAS campaign is available on the HALO database. As for the CARIBIC data, ERA5 reanalysis data including meteorological parameters and tropopause information were interpolated onto the PHILEAS flight tracks.

Quantification of the homogeneity of the data set due to dynamically induced variability can best be done by using a substance with clear characteristic of its atmospheric distribution and profile. In this study, we use focus on O_3 due to the well-understood and distinct atmospheric profile coupled with the ability to measure this substances with good precision at high resolution. O_3 data of CARIBIC and PHILEAS were obtained using a custom-built UV photometer with a typical uncertainty of 2% (or 2 ppb absolute) and a time series resolution of 0.25 Hz (Zahn et al., 2012; Obersteiner, 2024). The O_3 data from CARIBIC used here is part of the MS data set (Zahn et al., 2024), while the measurements during PHILEAS are available on the HALO Database (HALO, 2025).

3 Tropopause definitions

Multiple tropopause definitions fell in and out of favour over time with technological advancements and improved observation coverage (Gettelman et al., 2011). Table 1 shows an overview of the three main types of tropopause definitions that are in active use by the meteorological community, the advantages and disadvantages of each being the focus of this paper. Traditionally, the tropopause has been calculated using the temperature gradient obtained from atmospheric temperature profiles (WMO, 1957). Later, the ability to model dynamic processes on large scales allowed the formulation of dynamic tropopause definitions based on PV. Early proposals of a dynamic tropopause reference the isentropic gradient of PV, however for simplicity, dynamic tropopauses were largely adopted as constant PV surfaces. The PV gradient tropopause has gained more attention again through work of Kunz et al. (2011) and more recently by Turhal et al. (2024). Another approach discussed in Tinney et al. (2022) uses the gradient of potential temperature to define a tropopause similar to the temperature gradient, which was shown to identify

https://doi.org/10.5194/egusphere-2025-1589
Preprint. Discussion started: 24 April 2025

Table 1. Overview of commonly used tropopause definitions and their basis.

Definition	Based on:	Data from:
Thermal / WMO	Temperature lapse rate	Observations / Model
Dynamic	PV surface (e.g. 1.5, 2.0 or 3.5 PVU)	Model
Chemical: O_3 and N_2O	Climatology, tracer-tracer correlation, statistical baseline evaluation	Observations

sharper gradients in O_3 where these definitions do not coincide. For aircraft campaigns, the calculation of the distance to the local thermal and dynamic tropopauses relies on the availability of model data. This is due to vertical temperature profiles or potential vorticity curtains not being available in the data measured onboard.

With increasing availability of trace gas profiles through sondes and aircraft campaigns, the definition of chemical tropopauses became possible. The tropopause acting as a transport barrier, especially outside the tropics, results in steep gradients of some tracers in this region. Over the years, tracers such as O_3 (Bethan et al., 1996; Sprung and Zahn, 2010), N_2O (Assonov et al., 2013; Umezawa et al., 2014), or modelled tracers, for example the *e90* tracer with an e-fold decay time of 90 days, (Prather et al., 2011) have been used in literature with varying implementations. In concept, these chemical tropopauses are better able to identify small-scale structures and mixing events than modelled tropopauses which first have to be interpolated from lower temporal and spatial resolution model data.

For this work, thermal and dynamic tropopauses based on meteorological dynamic variables are calculated from ERA5 reanalysis data. The tropopause height and distance to the flight track are calculated for multiple vertical coordinates, such as pressure, geopotential height or potential temperature. Two separate approaches to define a chemical tropopause based on trace gas measurements are also presented.

3.1 Thermal tropopause

In the troposphere, the temperature generally decreases with increasing height, as less energy absorbed by the surface reaches higher air masses. This relationship, however, is inverted in the stratosphere. The definition of a *thermal* troposphere was officially formulated by the WMO (1957) with the following conditions:

1. Identify the lowest level at which the temperature lapse rate is below $2\,\mathrm{K\,km^{-1}}$.
2. The condition must be fulfilled that the average lapse rate between that level and all other higher levels within two kilometres does not exceed $2\,\mathrm{K\,km^{-1}}$.
3. Secondary or tertiary tropopauses may be identified if these conditions are met again at higher altitudes.

https://doi.org/10.5194/egusphere-2025-1589
Preprint. Discussion started: 24 April 2025

3.2 Potential vorticity-based tropopause

The PV value of an air parcel describes its capacity to rotate, thus giving information on the combination of dynamics and stratification of the atmosphere. Similarly to potential temperature, PV is conserved in frictionless and adiabatic flow. PV is defined as the dot product of stratification and absolute vorticity and its unit is the *potential vorticity unit* (PVU) defined as $\frac{10^{-6}\,\mathrm{K\,m^2}}{\mathrm{kg\,s}} \equiv 1\,\mathrm{PVU}$. Due to stratification above the tropopause, PV experiences a strong increase across the tropopause, allowing for the definition of a *dynamic* tropopause. While early proposals of PV-based tropopause definitions were focussed on the PV gradient, the vast majority of studies chose to present the dynamic tropopause using PV surfaces to simplify evaluating the tropopause. In 1986, the WMO identified 1.5 PVU as the ideal cut-off for the troposphere, although later studies found higher PV values to more accurately represent the tropopause. Throughout history, a variety of PV values have been used, with 1.5, 2.0 and 3.5 PVU standing out as the most commonly used thresholds; for a discussion see e.g. Hoerling et al. (1991). Furthermore, Kunz et al. (2011) found that the ideal PV threshold values may be different for the two hemispheres . The value of the PV threshold is correlated with the altitude of the tropopause, so that of these values, 1.5 PVU represents the lowest tropopause and therefore the strictest tropospheric criterion. The threshold values are positive in the northern hemisphere and negative in the southern hemisphere, as absolute vorticity changes sign. The dynamic tropopause is not defined near the equator, as (potential) vorticity experiences a singularity in that region. Consequently, the dynamic tropopause is often represented by a fixed value of potential temperature in the tropics, commonly set to 380 K, or alternatively combination with the thermal tropopause have been suggested (Wilcox et al., 2012). For this analysis, we focus only on extratropical observations north of 30°N.

3.3 Chemical tropopauses

As some longer-lived trace gases have a strong gradient across the tropopause, this characteristics of their vertical profile may be used to define a *chemical* tropopause. There are approaches using many different gas species and combinations thereof. This analysis will focus on two definitions: 1) using a mid-latitudinal climatology of O_3 to give the distance to the thermal tropopause and 2) a statistical baseline filter based on N_2O observations. By using chemical tropopauses over reanalysis data, the same data set may be used both for the definition of a tropopause as for the trace gas or parameter of interest. The mismatch between model resolution as well as the potential for modelled features to be slightly offset in location to observations can therefore be avoided. However, the use of chemical tropopauses is naturally limited by the availability of high-quality measurements.

3.3.1 Ozone-based tropopause

A typical vertical profile of O_3 can be characterised by a fairly well-mixed troposphere, a sharp gradient across the tropopause and increasing mixing ratios with height in the lower stratosphere. The profile is controlled by the mixing of descending O_3-rich stratospheric air and tropospheric air poor in O_3, leading to a consistent and strong increase within the LMS (Fischer et al.,

https://doi.org/10.5194/egusphere-2025-1589
Preprint. Discussion started: 24 April 2025

2000). Making use of the relative abundance in ozone sonde data in the last decades, O_3 observations can be used to find a distance between a climatological tropopause and the measurement point.

We use the chemical$_{O_3}$ tropopause as described in Sprung and Zahn (2010). Firstly, a climatology of O_3 data is created using sonde profiles from Hohenpeissenberg, linking O_3 mixing ratio to a position above the local thermal tropopause. This tropopause definition can then be applied to observational data by selecting the corresponding climatology per month. A measure of the distance to the tropopause is then obtained by finding the bracketing climatological values and interpolating the chemical$_{O_3}$ tropopause to the measured O_3 value. Note here that the relative altitude is not given for values below 60 ppb or results lower than 1.5 km below the tropopause, as the chemical$_{O_3}$ tropopause does not yield meaningful results for these values.

3.3.2 Nitrous Oxide-based tropopause

The greenhouse gas N_2O is emitted primarily by soil and oceans, whereas the main loss mechanism is photolysis in the stratosphere. In combination with the trace gas' life-time of 123 *(104-152)* years (SPARC, 2013), this results in the atmospheric profile of N_2O to have a well-mixed background in the troposphere, a strong cross-tropopause gradient in mid- and higher latitudes, and decreasing mixing ratios with increasing altitude in the stratosphere (Bisht et al., 2021). This characteristic profile allows the definition of a chemical tropopause based on N_2O measurements, where lower N_2O measurements are indicative of stratospheric air masses. Defining a chemical$_{N_2O}$ tropopause using trends measured at Mauna Loa, Umezawa et al. (2014) found this definition to be approximately equivalent to a dynamical tropopause with a 2.5 PVU threshold. Defining a tropopause based on N_2O observations has the benefit of being able to use the same observational data set as other substances at the focus of further study.

For this study, we separate stratospheric data from the tropospheric observations with higher mixing ratios using the statistical baseline filtering approach from Schuck et al. (2018). In an initial pre-flagging step, the iterative filter identifies and removes data points more than 3% lower than the respective tropospheric value by referencing background station observations. A tropospheric baseline is then fitted to the remaining points. Any measurements with mixing ratios further than 2 standard deviations below this fit are identified as stratospheric in origin. This process repeats until the limit criterion is reached, which we define as a change of less than 10% of the standard deviation of the baseline data compared to the previous iteration. By modifying this parameter, the chemical$_{N_2O}$ tropopause can be adjusted for a specific data set.

Similarly to a O_3-based tropopause, the chemical$_{N_2O}$ definition does not show sensitivity below the tropopause due to the well-mixed nature of these tracers in the troposphere. As the statistical baseline filter does not contain information on the vertical position of measurement, this tropopause can moreover not be expressed in traditionally used vertical coordinates such as height, pressure or potential temperature. This additionally hinders the study of parameters such as trends in the location of the tropopause or LMS mass. However, the difference between the N_2O value to its corresponding baseline can be treated as an

https://doi.org/10.5194/egusphere-2025-1589
Preprint. Discussion started: 24 April 2025

approximation for vertical displacement from the tropopause for some applications.

As for other tracer-based tropopause definitions, the chemical$_{N_2O}$ tropopause depends on how well a substance can be measured and the availability of the data. For this statistical filter to work properly, a significant fraction of the data needs to be tropospheric for the evaluation of a baseline. This could potentially be mitigated by careful combination of multiple data sets.

4 Results

4.1 CARIBIC data characterisation

To illustrate the differences between tropopause definitions, we first characterise the CARIBIC data set and its suitability for UTLS studies. In Fig. 1 the average seasonal distance of data points to the respective tropopause (Δz_{TP}) is shown. As the geopotential height of the flights does not vary considerably for all seasons and latitudes, the seasonal and latitudinal differences in Δz_{TP} are due to variations in the location of the tropopause. For all tropopauses, the sampling at lower latitudes can be characterised as more tropospheric. Overall, the distribution of measurement points shows that the CARIBIC data set is suitable for extratropical upper troposphere and lower stratosphere (exUTLS) studies due to significant sampling in the region around the tropopause in all seasons. The relationship between tropopause height and measurement points both in seasonality and latitudinal dependence varies between tropopause definitions. Here we use the geopotential height relative to the tropopause as vertical coordinate to compare the thermal, the three dynamic and the chemical$_{O_3}$ tropopauses.

The chemical$_{N_2O}$ tropopause is based on a statistical baseline filter based on the observed mixing ratio, which does not result in a clearly defined location of the tropopause. Instead, the difference between measurements and the baseline evaluated for that point in coordinates (the 'residual') is shown in Fig. 1 to give an approximate comparative value. In this plot, a negative difference indicates data points with lower N_2O than the baseline, which corresponds to a larger fraction of stratospheric air. One can see that neither the seasonal average nor its standard deviation go significantly below zero, which shows the absence of downward sensitivity for this tropopause definition. The chemical$_{N_2O}$ tropopause data shown in Fig. 1 therefore mainly shows the seasonality of stratospheric measurements in the CARIBIC data set, while the tropospheric data has a smaller impact on these values. Notably, the chemical$_{N_2O}$ presents very differently to other tropopause definitions, with the displacements in summer being close to the average, while the thermal and dynamic definitions then result in lower Δz_{TP} than other seasons.

Figure 1 also shows that the distribution of measurement points at higher latitudes is in agreement for the dynamic$_{3.5}$ and the thermal tropopause. In this region, the seasonality of the thermal and dynamic definitions follows the same overall structure, where flight paths are closest to the lower lying tropopause in summer. The difference between distributions using dynamic tropopauses with different thresholds is evident mostly through a vertical displacement, while the seasonality and latitudinal trends are very similar. Towards low latitudes, the thermal tropopause results in larger seasonal differences than the dynamics

https://doi.org/10.5194/egusphere-2025-1589
Preprint. Discussion started: 24 April 2025

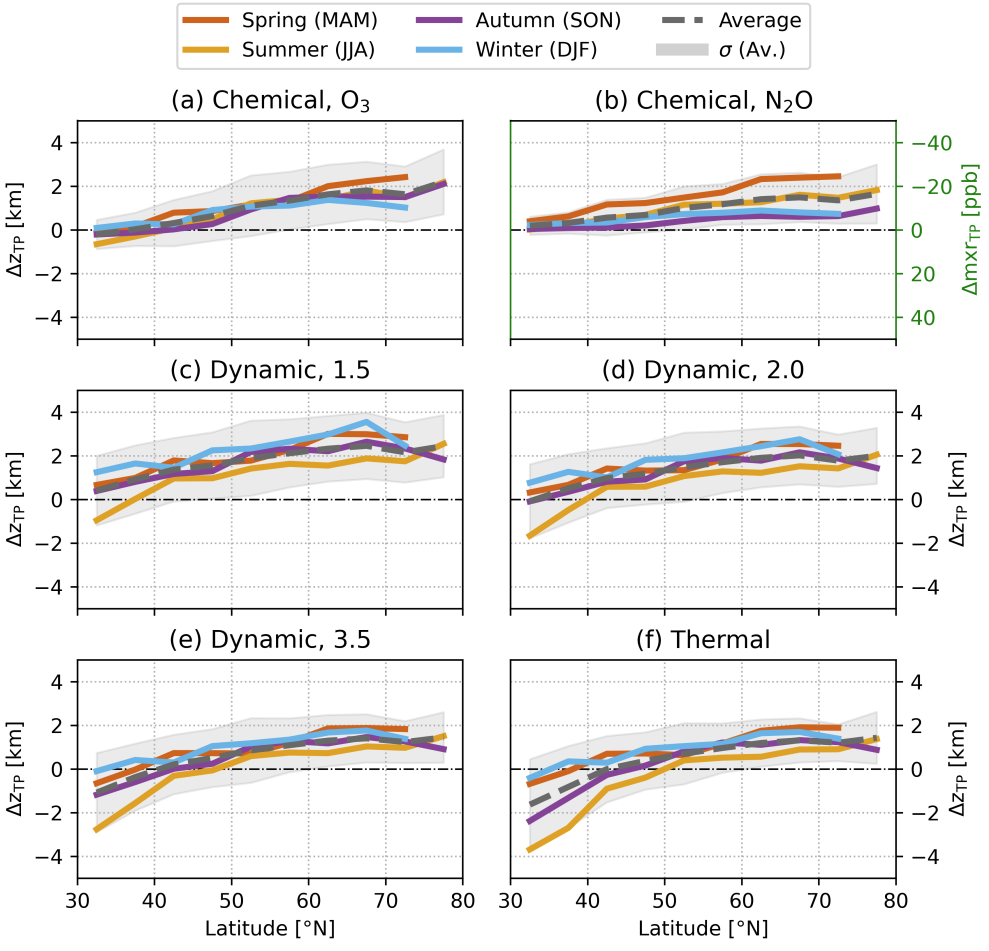

Figure 1. Latitude-binned (5°) mean distance of whole-air-sampler measurements to the respective tropopause across the whole CARIBIC measurement period. Panels (a) and (b)–(f) show the distance in geopotential height, while in panel (b) the difference between N_2O observations and the statistically evaluated baseline of the chemical$_{N_2O}$ is given. The grey shading indicates the standard deviation of the seasonal average.

definitions, with the average distance between measurements and the tropopause ranging from less than one to almost four kilometres below the tropopause. In this region, the influence of the subtropical jet (STJ) is expected to lead to dynamic changes which may not be well represented by the temperature gradient.

In contrast, both chemical tropopause definitions result in significantly lower seasonal variability at mid-latitudes. This is likely in large part due to sampling bias, as the flight path height relative to the tropopause is not meaningful for ozone values below 60 ppb. In this comparison, the chemical tropopauses therefore exhibit a lower variability at lower latitudes, as the remaining data set is more homogenous regarding mixing ratios. Other tropopause definitions result in higher variability in this

https://doi.org/10.5194/egusphere-2025-1589
Preprint. Discussion started: 24 April 2025

region, as the calculation of average distance between flight track and tropopause is independent on the ozone mixing ratio and therefore less sensitive to this filtering bias. In the CARIBIC data set, this effect is weakest at higher latitudes, where the flight path is on average higher above the tropopause.

At high latitudes, the chemical$_{O_3}$ tropopause tends to be closer to the flight track in winter and further away in spring, while the summer and autumn values stay close to the average displacement. We believe the difference in seasonality between chemical$_{O_3}$ and thermal/dynamic tropopauses to be an effect of using a mid-latitudinal ozone climatology to calculate the chemical$_{O_3}$ tropopause. Using ozone observations to find the displacement to the tropopause in the polar regions through comparison to a mid-latitudinal climatology is likely to result in an underestimation of the displacement to the tropopause in high latitudes in winter.

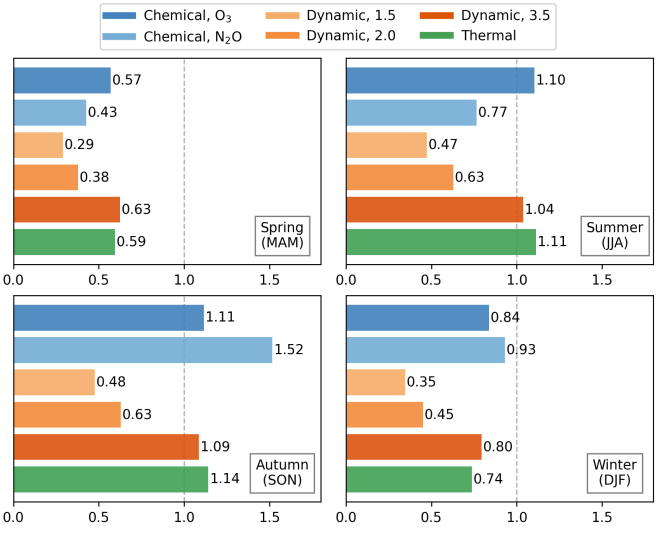

Figure 2. Tropospheric fraction per season as identified by different tropopause definitions in the CARIBIC data set 2005-2020 on whole-air-sampler time resolution. A fraction of 1 indicates an even split of tropospheric and stratospheric measurements.

As a consequence of the high number of data points around the tropopause and varying tropopause heights, the total number of data points in the troposphere or stratosphere varies significantly between tropopause definitions. Depending on the definition, the total share of tropospheric data points ranges from 29 % to 48 %. Figure 2 shows that the ratios are statistically in good agreement for all seasons between the thermal, dynamic$_{3.5}$ and chemical$_{O_3}$ tropopauses. There are some slight differences between these definitions, most notably a larger fraction of tropospheric air for the dynamic$_{3.5}$ tropopause in winter and a larger stratospheric fraction for the chemical$_{O_3}$ tropopause in spring, but the overall seasonal trends are very similar. Note here that the chemical$_{O_3}$ tropopause is not completely independent of the thermal tropopause: As outlined in Sect. 3.3.1 , the climatology of the chemical$_{O_3}$ definition is calculated as a distance to the thermal tropopause. While the differences between tropopauses

https://doi.org/10.5194/egusphere-2025-1589
Preprint. Discussion started: 24 April 2025

seasonalities are small, they may be an indication of different sensitivities of specific definitions to seasonal changes in the atmosphere, for example diabatic transport processes. Following from the displacement of the vertical tropopause location in the atmosphere, the tropospheric ratios obtained for different dynamic tropopauses decrease with lower PVU-thresholds. Of each data point identified as tropospheric by the dynamic$_{3.5}$ tropopause, only 70 % are also below the dynamic$_{2.0}$ tropopause and 61 % below the dynamic$_{1.5}$ tropopause.

It is expected that with careful choice of the corresponding threshold values, the dynamic tropopause should coincide with trace gas-based definitions. This is because trace gas distributions roughly follow surfaces of adiabatic frictionless flow, which the dynamic tropopause represents. As the meteorological variables are calculated as part of a global model, however, small features may either not be resolved or appear slightly offset from the measured atmospheric dynamics. Moreover, Fig. 2 shows that while the two tracer-based definitions resulted in similar seasonalities of Δz_{TP} over latitude, the seasonality of tropospheric fractions presents quite differently for the two chemical tropopauses.

While the chemical$_{O_3}$ tropopause results in a similar tropospheric ratio as the thermal and dynamic$_{3.5}$ tropopauses, with the chemical$_{N_2O}$ a much larger number of data points are identified as tropospheric in autumn. The ratios obtained using the chemical$_{N_2O}$ tropopause exhibit a much stronger seasonality than other tropopause definitions, with only 30.1 % of data points in spring identified as tropospheric, compared to 60.5 % in autumn. This increased tropospheric fraction is likely due to the weakening of the subtropical jet and tropical air consequently being flushed into the extra-tropics. This then results in lower N_2O mixing ratios than the northern hemispheric background, an effect which propagates into winter.

To check for biases in the WAS data set, we repeat this analysis with the high resolution CARIBIC data on 10 s timestamps as well as for the 40-60°N latitude subset. We find that these results are in agreement with the low-resolution analysis both in overall tropospheric ratios and seasonal trends. A comparison between potential temperature differences between flight track and dynamic/thermal definitions results in the same overall trends for seasonality and latitudinal dependence. In this coordinate system, however, the differences between seasons are not dependent on the latitude to the same extent as with geopotential height. We continue using WAS timestamps and geopotential height for the following analyses to allow the use of both the N_2O measurements and the height-based chemical$_{O_3}$ tropopause data.

4.2 Homogeneity of vertical distributions

We now use ozone observations to investigate how well trace gas distributions across the atmosphere are characterised using different tropopause definitions. Figure 3 shows interpolated CARIBIC ozone data sorted into troposphere and stratosphere. Note that a large number of observations with very high O_3 mixing ratios are sorted as tropospheric using the thermal tropopause. The influence of higher ozone measurements sorted into the troposphere leads to a higher variability of potential temperature bins, which are here indicated through horizontal bars. In contrast, lower PV-thresholds of the dynamic tropopause result in a

https://doi.org/10.5194/egusphere-2025-1589
Preprint. Discussion started: 24 April 2025

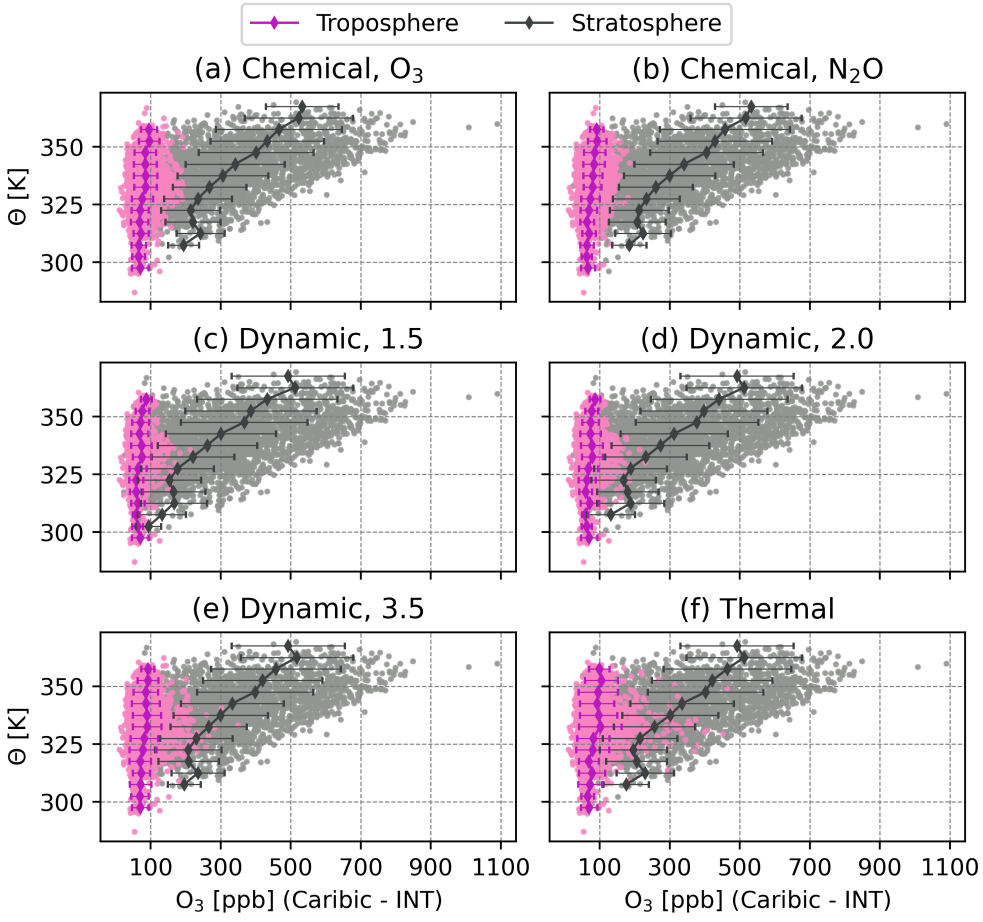

Figure 3. Ozone mixing ratios over potential temperature sorted into tropospheric and stratospheric air using different tropopause definitions. The average measurement values and standard deviation are shown for each potential temperature (5 K) interval.

reduction in the number of tropospheric points, which leads to lower mean O_3 and variability per potential temperature bin. The dynamic$_{1.5}$ and dynamic$_{2.0}$ tropopauses however also result in sorting a significant number of observations with low ozone mixing ratio into the stratosphere.

To evaluate the effectiveness of grouping homogeneous air masses by different tropopause definitions, we explore the variability of vertical profile bins in more detail. Similar to before, ozone measurements are identified as either tropospheric or stratosphere, however now they are binned on a grid of geopotential height (0.5 km) and latitude (1° N). For each bin containing more than 5 data points, the variability of those observations is calculated. To evaluate which tropopause definitions results in better homogenisation of the ozone data, i.e. an overall lower binned variability, we show the frequency distribution of variabilities in Fig. 4. The distributions can roughly be quantified by applying a log-normal fit. The fitted curves as well as the mode

https://doi.org/10.5194/egusphere-2025-1589
Preprint. Discussion started: 24 April 2025

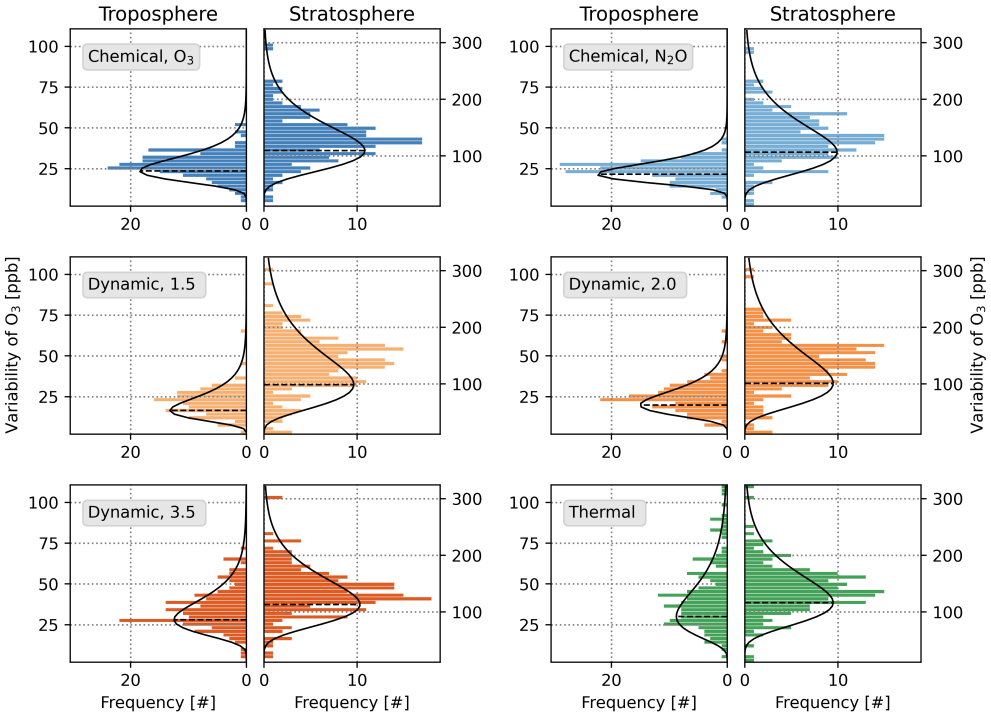

Figure 4. Distribution of tropospheric and stratospheric variability of CARIBIC ozone data. Measurements are separated using different tropopause definitions and binned onto a grid of latitude (1° N) and geopotential height (0.5 km). The distribution of variability of the resulting bins is shown as a histogram with log-normal fit applied to it. The mode of the distribution is indicated by a dashed line leading to the peak of the fitted curve.

of the resulting fit are indicated by the black lines. In an idealised case, the distribution would be dominated by the natural variability of ozone with a minimisation of the variability introduced by changes in tropopause height. In the troposphere, we expect lower variability values for definitions that are more effective in filtering out stratospheric data points.

The results of this log-normal fit of variability distributions for all seasons and tropopause definitions is shown in Fig. 5. While the overall number of tropospheric data points is similar for the thermal, dynamic$_{3.5}$ and chemical$_{O_3}$ tropopauses, clear differences exist in the binned variability. For all seasons, the tropospheric bin variability of ozone is largest with the thermal tropopause and decreases with lower PV-thresholds, which correspond to fewer data points sorted into the troposphere overall. The chemical$_{N_2O}$ tropopause results in relatively broad distributions of variability in autumn and winter, which likely follows from the higher tropospheric fraction in these seasons than other tropopause definitions.

The influence of chemical processes and much higher mixing ratios leads to a larger natural variability of ozone in the stratosphere. The stratospheric variability distributions are therefore much less sensitive to differences between tropopause definitions. Figure 5 however clearly shows the reduced variability of ozone in autumn and higher variability in spring and

https://doi.org/10.5194/egusphere-2025-1589
Preprint. Discussion started: 24 April 2025

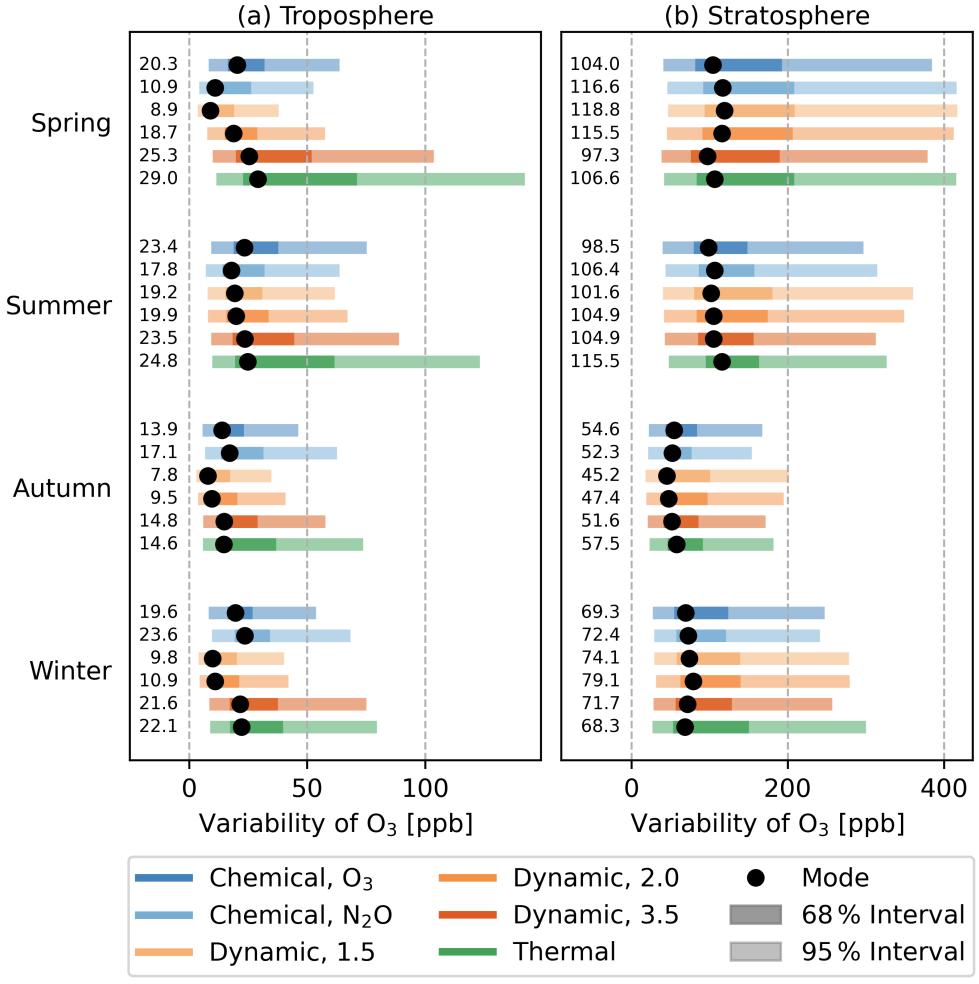

Figure 5. Mode and 68/95% interval widths of log-normal fit on distribution of variability in 2D-binned O_3 measurements on WAS resolution. Binning was carried out for each season in latitude (1°) x geopotential height (0.5 km). The distribution is shown for (a) the troposphere and (b) the stratosphere as identified by different tropopause definitions. The large dots indicate the mode of the variability distribution while the shading shows the 68% and 95% intervals of the log-normal fit.

summer. For an alternative representation, the variabilities of binned ozone data are also shown in coordinates relative to the tropopause in Appendix A.

4.3 Vertical profiles and cross-tropopause gradient

The previous sections have shown that there are significant differences between tropopause definitions even in coordinates such as potential temperature or geopotential heights. To further explore these differences, we now investigate the impact when us-

https://doi.org/10.5194/egusphere-2025-1589
Preprint. Discussion started: 24 April 2025

ing tropopause-relative coordinates. Figure 6 shows that the cross-tropopause gradient of O_3 is strongest in spring and summer and weakest in autumn and winter for all tropopause definitions with a clearly defined vertical coordinate.

The chemical$_{N_2O}$ tropopause in Fig. 6b) is shown using the difference between N_2O mixing ratio to the statistically evaluated baseline for each measurement. While this coordinate gives some information on the vertical position of the measurement point, this representation does not show the seasonality of the ozone vertical profile in the way other tropopause definitions do, but rather the correlation between O_3 and N_2O. One can see that the correlation does not have a significant seasonality, however the variability of O_3 vs. ΔN_2O strongly increases in winter.

All other tropopause definitions show clear seasonal trends in mean mixing ratios in troposphere and stratosphere. The overall ozone mixing ratio at a given height above the tropopause is lowest in autumn and winter and highest in summer and spring, with a qualitatively similar seasonality in the troposphere. The seasonal differences tend to become more pronounced the deeper in the stratosphere the measurements are being taken. While there is a clear separation between seasons for the thermal and dynamic definitions, the winter and summer profiles resulting from the chemical$_{O_3}$ tropopause are similar in value. Overall, the seasonal vertical profiles are alike for the dynamic and thermal tropopauses.

The variability in the tropospheric bins tends to be smaller for all definitions than in the stratosphere. As before, this is due to overall much higher mixing ratios in the stratosphere as well as chemical processes introducing natural variability. For the chemical$_{O_3}$ tropopause, however, the variability in spring and autumn are much smaller than other tropopause definitions higher above the tropopause. The variability is highly impacted by the use of ozone both as the basis for calculating the tropopause as well as substance at the focus for this analysis and can therefore not be directly compared.

The gradient of trace gases across the tropopause can be used as a measure of how well a given definition characterises the transport barrier. A stronger gradient indicates a sharper transition between troposphere and stratosphere, reflecting a clearer separation between tropospheric and stratospheric data. In Fig. 7 we compare the cross-tropopause gradient of ozone between tropopause definitions, which are also highlighted in the small panels in Fig. 6. The gradient is first expressed as mixing ratio difference per vertical coordinate unit. Then, this value is normalised to the average ozone mixing ratio at the tropopause for that season. Here we are evaluating the gradient using binned data up to 0.5 km above and below the tropopause. The parameters used for the calculations and normalisations are given in Appendix B.

The largest ozone mixing ratios in the stratosphere are present in spring and summer, which leads to stronger cross-tropopause gradients. While the northern-hemispheric tropospheric average also changes slightly between seasons and is elevated in spring, most definitions also identify the strongest gradients in this season. The overall highest gradient, however, is presented by the dynamic$_{3.5}$ tropopause in summer. The gradient is weakest in autumn for all definitions except the thermal tropopause, which presents similarly for summer and autumn. Overall, the dynamic$_{3.5}$ tropopause results in the strongest

https://doi.org/10.5194/egusphere-2025-1589
Preprint. Discussion started: 24 April 2025

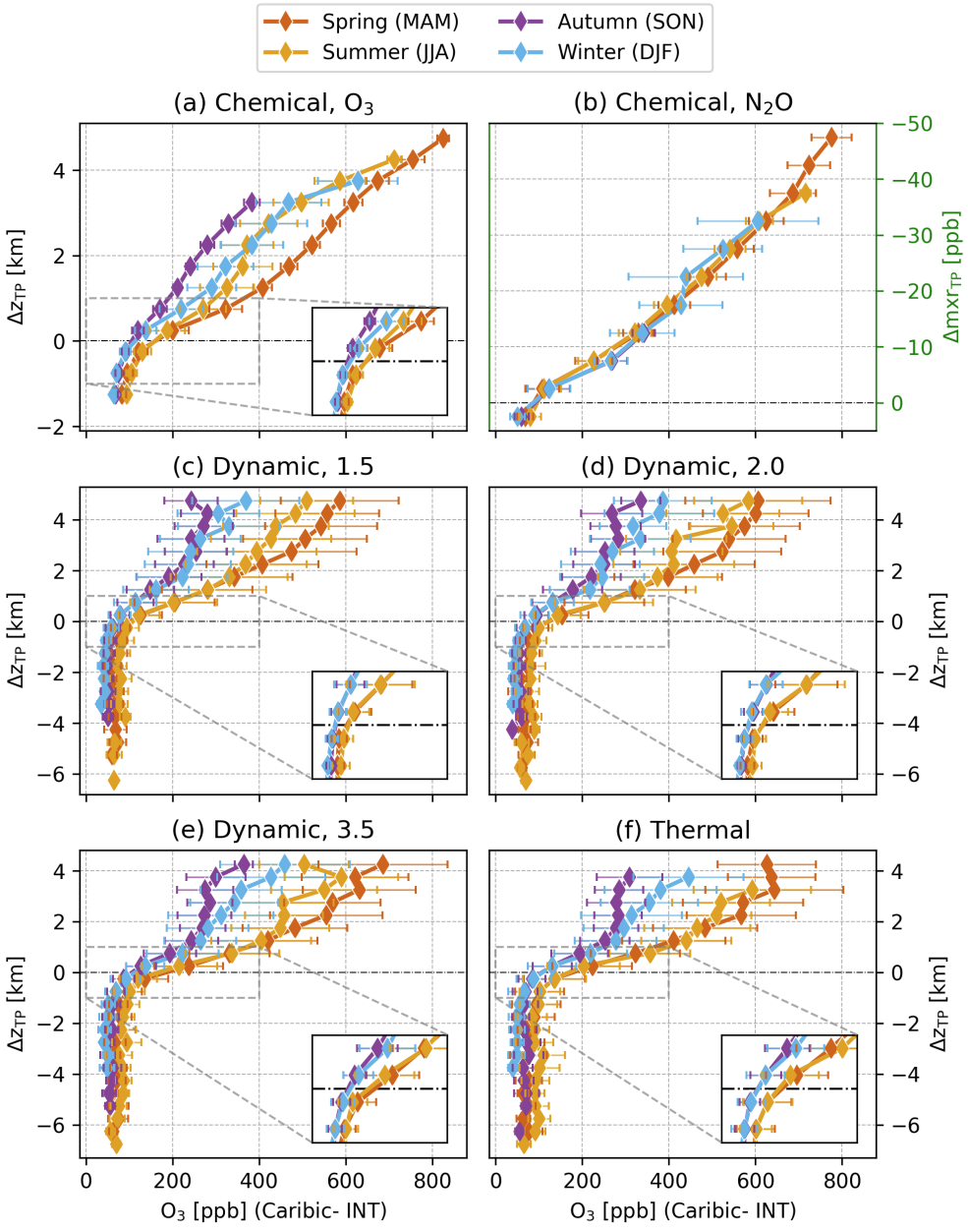

Figure 6. Seasonal vertical profiles of CARIBIC O_3 mixing ratios showing the distance relative to the tropopause for six definitions. The standard deviation of each bin is indicated by the error bars. The coordinates for panels (a) and (c) through (f) are geopotential height, while panel (b) shows the difference between the corresponding N_2O measurement and the statistically evaluated baseline value. Extra panels show the region of ± 1 km around the tropopause and ozone mixing ratios of 0–400 ppb.

https://doi.org/10.5194/egusphere-2025-1589
Preprint. Discussion started: 24 April 2025

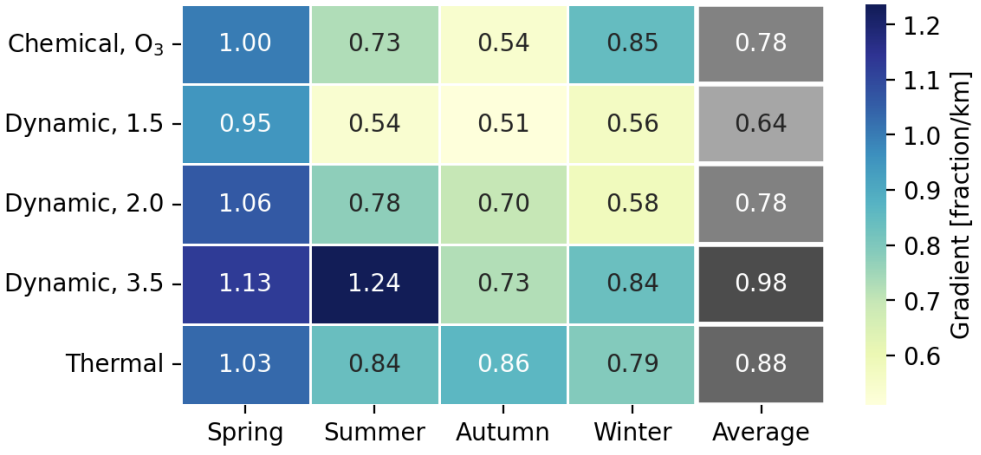

Figure 7. Climatological normalised cross-tropopause gradient of ozone across ±0.5 km of the indicated tropopauses. The values are normalised to the average seasonal value at the respective tropopause. Large gradients represent sharp gradients across the tropopause.

seasonal gradients and identifies the sharpest gradients. The thermal tropopause identifies the second strongest gradients, with a weaker seasonality than other definitions. The chemical$_{O_3}$ and dynamic$_{2.0}$ tropopauses return a similar average gradient, however the chemical$_{O_3}$ returns a much higher cross-tropopause gradient in winter.

Since the mixing ratio of ozone increases with height in the stratosphere, it is possible to calculate high cross-tropopause gradients for tropopause definitions well above the transition between well-mixed troposphere and stratosphere too. Care must therefore be taken to take into account that a tropopause definition should not only return large cross-tropopause gradients, but that the gradient of the bins just below the tropopause should be relatively small. In Appendix C the gradients below the tropopause as well as the difference to the gradient at the tropopause are shown. The dynamic$_{3.5}$, thermal and chemical$_{O_3}$ overall have similar gradients in the bins just below the tropopause, which are higher than for the dynamic tropopauses at lower PV thresholds. However, the mean seasonal gradients in these bins reach a maximum of 0.43 when normalised to the same value as the gradient at the tropopause, which is more than a factor of 2 smaller than the cross-tropopause gradient for the same tropopause and season. As presented in Appendix D, for the CARIBIC data, the 2.0 and 1.5 PVU thresholds result in average tropopause heights 0.7 and 1.0 km lower than the dynamic$_{3.5}$ definition, respectively. The weaker gradients across the tropopause are therefore indicative of a systematic lower mapping of tropopause heights to altitude than strong gradients with these thresholds. On the other hand, while the thermal tropopause results in relatively strong cross-tropopause gradients, the difference to the gradient just below the tropopause is not as strong as other definitions, especially in summer. With an average height 0.27 km above the dynamic$_{3.5}$ tropopause in summer, this shows a higher mapping of thermal tropopause height in this season.

https://doi.org/10.5194/egusphere-2025-1589
Preprint. Discussion started: 24 April 2025

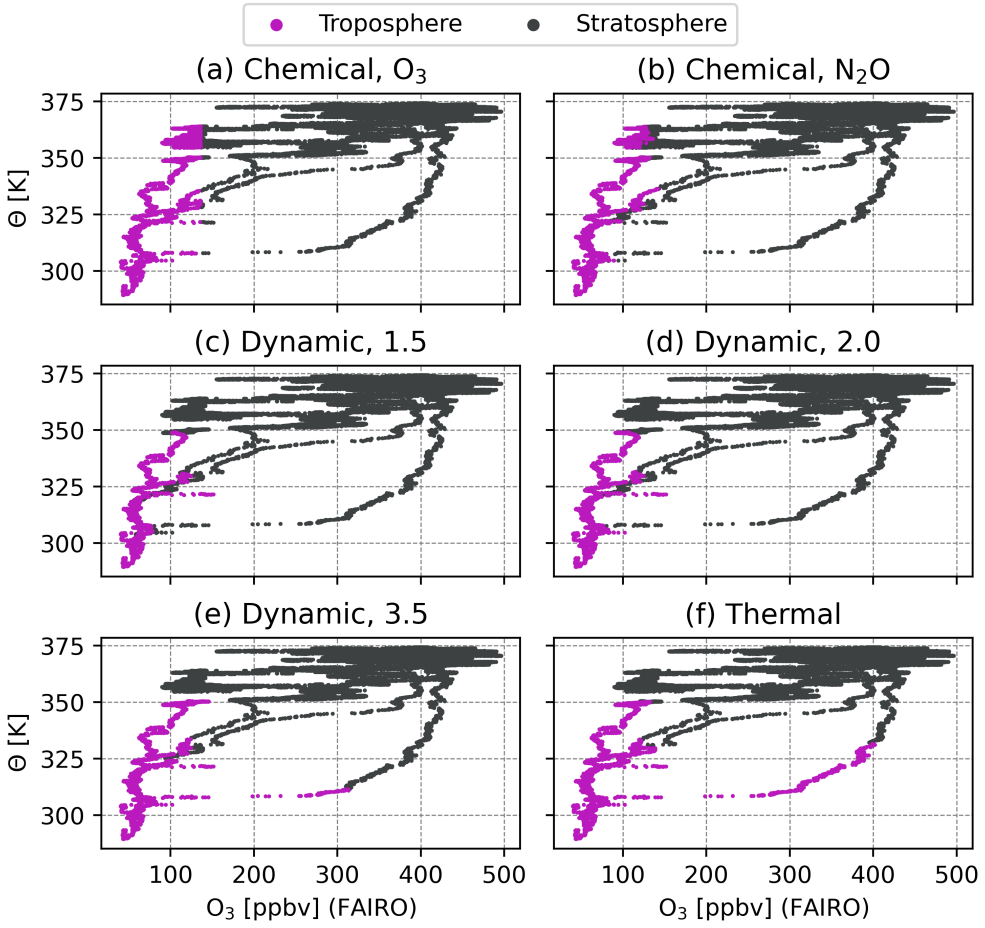

Figure 8. Ozone measurements taken during PHILEAS on 21 August 2023 from Munich to Anchorage over potential temperature. Data points are sorted into troposphere and stratosphere using different tropopause definitions, which is indicated by the colour.

4.4 Case studies - features in small data sets

To verify the conclusions drawn from the climatological analysis in the last sections, we now investigate individual flights with high resolution N_2O and O_3 data from the HALO campaign PHILEAS. We focus on the two transfer flights between Germany and Alaska on 21 August and 22 September 2023, which were chosen due to the large longitudinal range coverage and because they did not set a special focus on exploring atmospheric features. The same processing as before is applied to the data, with ERA5 reanalysis parameters being interpolated onto the flight path and the statistical baseline filter being applied to N_2O observations.

https://doi.org/10.5194/egusphere-2025-1589
Preprint. Discussion started: 24 April 2025

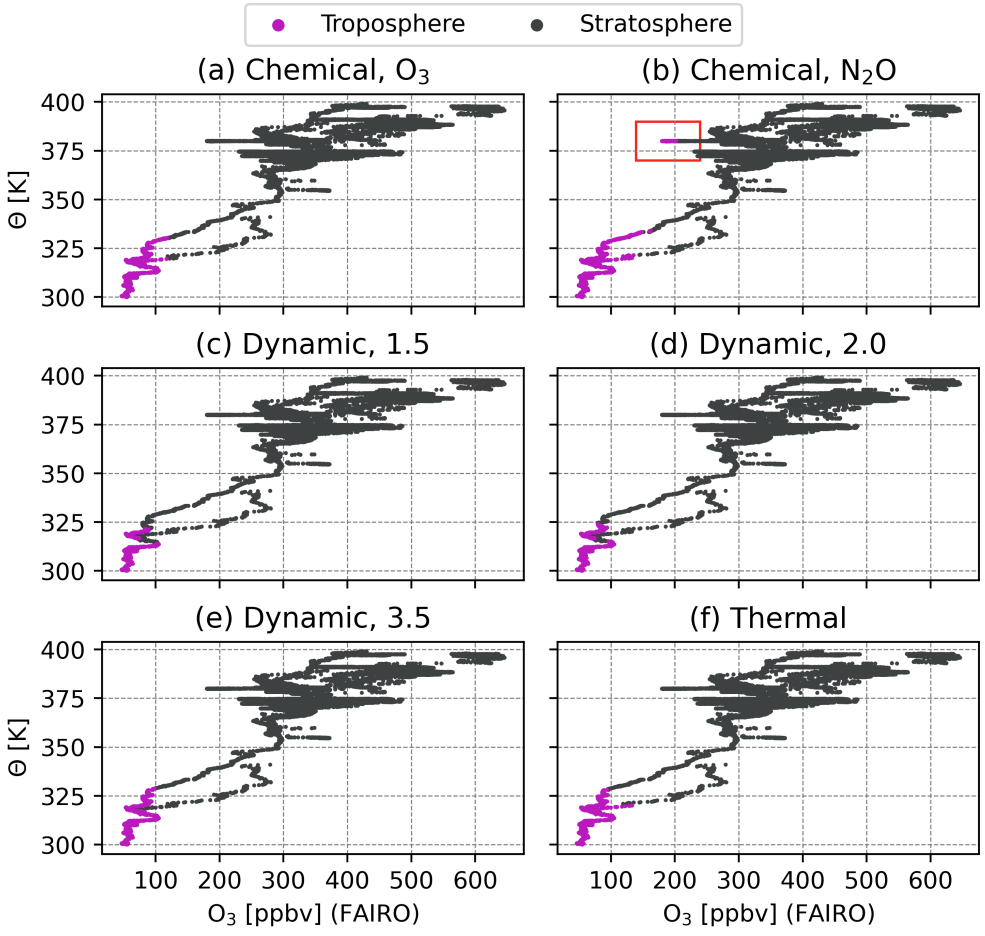

Figure 9. As Fig. 8 for PHILEAS on 22 September 2023 from Anchorage to Munich. A number of points identified as tropospheric by the chemical$_{N_2O}$ tropopause is highlighted in the top right panel.

Figure 8 shows data from the transfer between Germany to Alaska. The overall shape of the correlation of ozone observation to absolute PV is positive, however there is a distinct feature with low potential temperature and increasing ozone mixing ratio with V. The sorting of tropospheric and stratospheric data within this feature is significantly different for different tropopause definitions: While the chemical and dynamic tropopauses agree on the stratospheric sorting of the measurements with very high ozone (>300 ppbv) and high PV (>5 PVU), this feature does not appear to be resolved in the thermal tropopause. Using the dynamic$_{1.5}$ and dynamic$_{2.0}$ tropopauses gives a stratospheric identification for all of these high ozone mixing ratio values, while the dynamic$_{3.5}$ tropopause leads to large parts of this feature to be sorted into the troposphere due to a higher PV-threshold.

https://doi.org/10.5194/egusphere-2025-1589
Preprint. Discussion started: 24 April 2025

In the next example shown in Fig. 9, we look at the transfer flight from Alaska to Germany. Here, we see the same overall correlation between high PV values and high ozone observations. While all tropopause definitions approximately agree that the majority of measurements were taken in the stratosphere, a collection of points with high potential temperature, ozone mixing ratio of about 200 ppbv and high PV stands out. These measurements were identified as tropospheric by the chemical$_{N_2O}$ tropopause but no other definition. This may be caused by the overall very low number of tropospheric points in this data, which hinders the identification of a meaningful tropospheric baseline.

5 Conclusions

Using the IAGOS-CARIBIC data set and selected flights from the PHILEAS campaign onboard HALO, we compared six commonly used tropopause definitions: The thermal tropopause based on the temperature lapse rate, dynamic tropopauses based on the 1.5 PVU, 2.0 PVU and 3.5 PVU thresholds, and chemical tropopauses based on either a climatology of O_3 or a statistical baseline approach using N_2O. We found that overall the number of measurement points identified as tropospheric varies little between chemical$_{O_3}$, dynamic$_{3.5}$ and the thermal tropopause, however the chemical$_{N_2O}$ shows a much stronger seasonality. Dynamic tropopauses with a PV-thresholds of 1.5 PVU or 2.0 PVU are very effective at filtering out stratospheric data, with the potential disadvantage of filtering out some tropospheric data points close to the tropopause too.

Characterising the variability of ozone in the troposphere showed that the thermal tropopause does not effectively filter out stratospheric data from the CARIBIC data set. The lower number of tropospheric points in the low PV tropopauses resulted in overall reduced variability. An analysis of the cross-tropopause gradients also showed overall weaker gradients for these tropopauses due to an overall lower mapping of the tropopause to height and associated lower O_3 mixing ratios across the tropopause. The strongest cross-tropopause gradients were found using the dynamic$_{3.5}$ tropopause, indicating the strongest climatological representation of the tropopause transport barrier. On the other hand, using the thermal tropopause results in a larger number of high O_3 observations in the troposphere, leading to a weaker gradient across the tropopause than the dynamic$_{3.5}$ definition for all seasons. The chemical$_{O_3}$ tropopause returned similar gradients as the dynamic$_{2.0}$ definition. There are slight seasonal differences between definitions, however the strongest cross-tropopause ozone gradient was found in spring and the weakest one in autumn for all tropopauses.

In analysing smaller data sets, we found benefits of using chemical tropopauses based on in-situ data over the modelled tropopauses. Especially in the case of a small-scale feature with high ozone and low potential temperature, the thermal and dynamic$_{3.5}$ tropopause identified points as tropospheric contrary to all other definitions. However, difficulties in applying the chemical$_{N_2O}$ definitions were shown in another example, where the low fraction of tropospheric observations lead to a feature of very high potential temperature and elevated O_3 mixing ratio to be identified as tropospheric. Care must therefore be taken

https://doi.org/10.5194/egusphere-2025-1589
Preprint. Discussion started: 24 April 2025

in choosing suitable data sets and sensible input parameters.

To conclude, we find that in the extra-tropics, the commonly used threshold value of 2.0 PVU maps the tropopause height to a lower altitude than where the strongest ozone gradients are situated. We find the dynamic$_{3.5}$ definition to best represent the transport barrier of the tropopause without introducing additional variability to the tropospheric part of the data set, although small features may not be resolved in large-resolution reanalysis data. Chemical tropopauses were shown to work effectively in reducing tropospheric variability. However, the chemical$_{O_3}$ definition resulted in weaker cross-tropopause gradients than the thermal and dynamic$_{3.5}$ tropopauses. As our analysis of the chemical$_{N_2O}$ definition was hindered by the lack of comparable vertical coordinate, we recommend further investigation in formulating a similar framework as for the chemical$_{O_3}$ tropopause. We also suggest future implementations of climatology-based chemical tropopauses to be presented using potential temperature distances to the dynamic tropopause, instead of height relative to the thermal tropopause. For such implementations, we recommend that climatologies be evaluated for several latitude bands. We further highlight the importance of high-resolution O_3 and N_2O data onboard aircraft campaigns as well as global coverage of these substances at ground-level.

Data availability. The whole-air-sampler data of the IAGOS-CARIBIC project are available at 10.5281/zenodo.8188548, the merged (MS) high resolution IAGOS-CARIBIC data at https://zenodo.org/records/14000090. The observational data of the HALO flights during the PHILEAS campaign are available via the HALO database (https://halo-db.pa.op.dlr.de/mission/138).

Author contributions. TS operated and provided data of the CARIBIC air sampler; AZ and FO operated and provided data of the CARIBIC-O_3 and FAIRO instruments; NE, PH, LO, and FW operated and provided data of the UMAQS instrument; and HCL contributed the ERA5 model data interpolated to the flight track . SB, TS and AE initiated and conceptualised the core research goals and together with HB and PH contributed valuable ideas in discussions. SB performed the analyses and prepared the manuscript with contributions from TS and AE. All authors contributed via discussion and comments.

Competing interests. At least one of the (co-)authors is a member of the editorial board of Atmospheric Chemistry and Physics.

Acknowledgements. This research has been supported by the Deutsche Forschungsgemeinschaft (grant no. SCHU 3258/3-1 – project ID 501095243) and DFG collaborative research programme “The Tropopause Region in a Changing Atmosphere” TRR 301 – project ID 428312742). This research was supported by the German Research Foundation (DFG) within the Priority Program HALO SPP 1294 under project number 316646266 and EN 367/19-1. IAGOS-CARIBIC data were created with support from the European Commission, national agencies in Germany (BMBF), France (MESR) and the UK (NERC), and the IAGOS member institutions (https://www.iagos.org/organisation/members).

https://doi.org/10.5194/egusphere-2025-1589
Preprint. Discussion started: 24 April 2025

Appendix A: Variability distribution of O_3 in CARIBIC

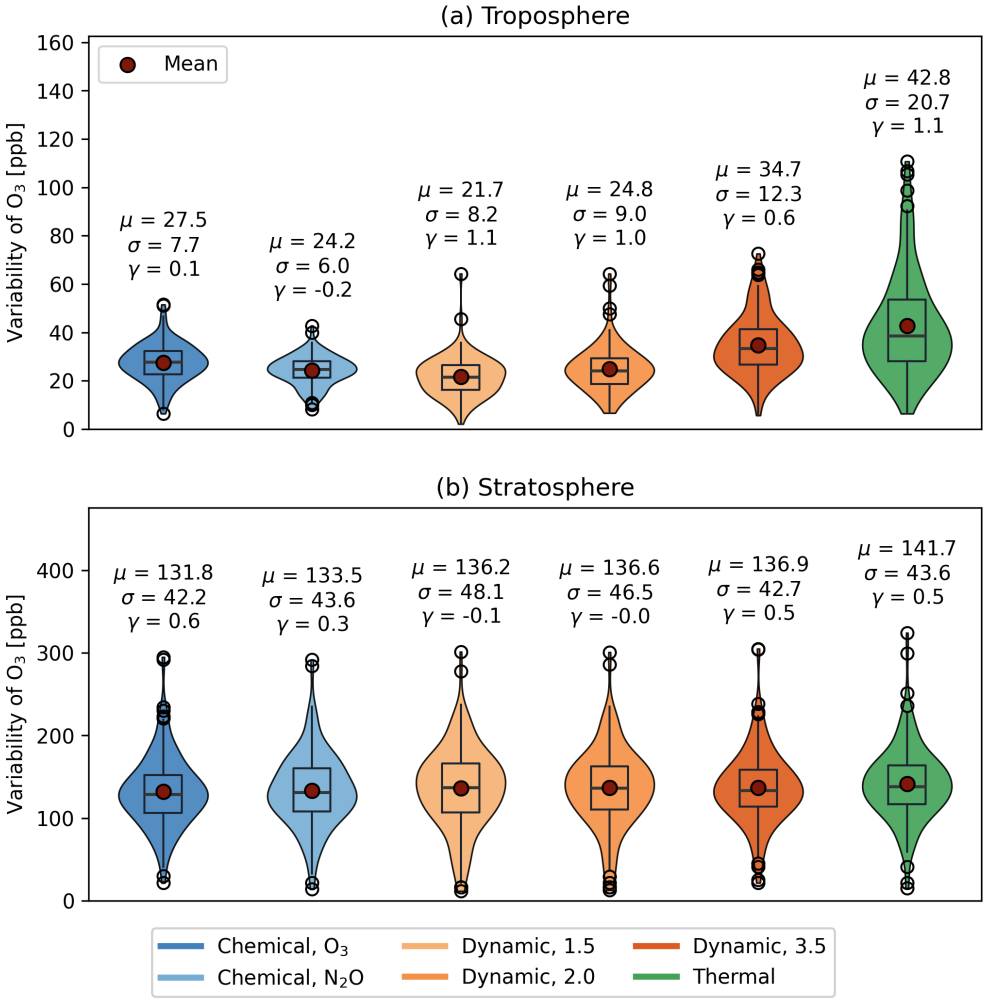

Figure A1. Distribution of tropospheric and stratospheric variability of binned CARIBIC ozone data. Measurements are separated using different tropopause definitions and binned onto a grid of latitude (1° N) and geopotential height (0.5 km). The statistical parameters describing the distributions are the mean (μ) [ppb], standard deviation (σ) [ppb] and skewness (γ) [-].

https://doi.org/10.5194/egusphere-2025-1589
Preprint. Discussion started: 24 April 2025

Appendix B: Cross-tropopause gradient parameters

Table B1. Cross-tropopause gradient parameters for ozone in CARIBIC data. Ozone data is first binned in 0.5 km steps around the tropopause, then average values of those bins are evaluated. The difference between them over the step size of 0.5 km gives the gradient, which is then normalised to the value at the tropopause ± 0.25 km. All values are mixing ratios.

Tropopause definition	Season	Below TP [ppb]	Av. at TP [ppb]	Above TP [ppb]	Gradient [ppb/km]	Gradient [fraction/km]
Chemical_{O_3}	Spring	121.11	158.32	200.29	158.36	1.00
	Summer	130.70	156.51	187.60	113.81	0.73
	Autumn	91.68	104.64	120.03	56.70	0.54
	Winter	90.42	111.67	137.71	94.57	0.85
$\text{Dynamic}_{1.5}$	Spring	80.20	96.83	126.16	91.93	0.95
	Summer	94.51	102.53	122.10	55.18	0.54
	Autumn	61.81	67.80	79.13	34.64	0.51
	Winter	58.55	68.02	77.77	38.43	0.56
$\text{Dynamic}_{2.0}$	Spring	92.74	114.44	153.54	121.60	1.06
	Summer	98.80	114.27	143.17	88.73	0.78
	Autumn	67.65	76.78	94.42	53.55	0.70
	Winter	67.68	76.99	90.17	44.97	0.58
$\text{Dynamic}_{3.5}$	Spring	135.53	180.84	237.46	203.87	1.13
	Summer	120.36	153.27	215.16	189.60	1.24
	Autumn	87.23	109.16	126.84	79.21	0.73
	Winter	91.24	110.15	137.25	92.03	0.84
Thermal	Spring	135.55	168.98	222.96	174.83	1.03
	Summer	136.09	160.41	203.34	134.50	0.84
	Autumn	84.05	107.78	130.64	93.17	0.86
	Winter	87.25	109.13	130.52	86.54	0.79

https://doi.org/10.5194/egusphere-2025-1589
Preprint. Discussion started: 24 April 2025

Appendix C: Gradient of O_3 below the tropopause.

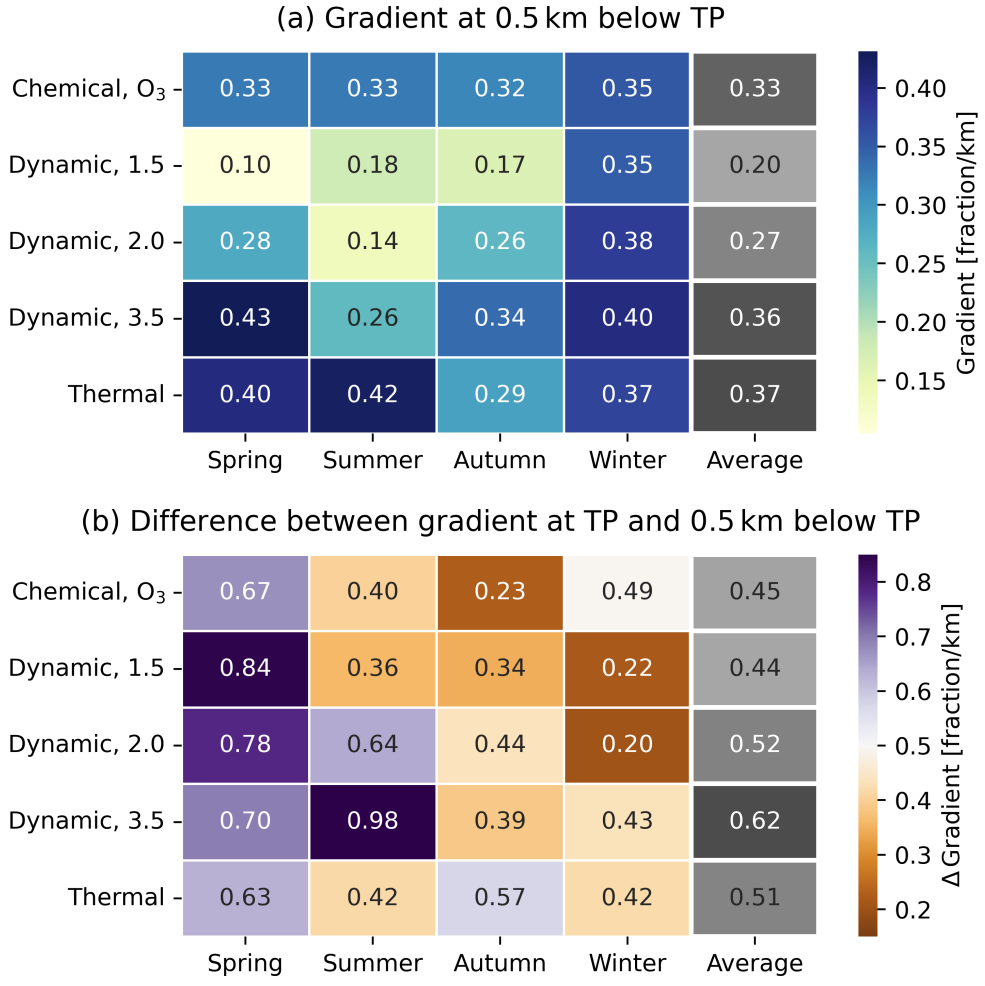

Figure C1. a) Normalised O_3 gradient 0.5 km below the tropopause. Higher values indicate the presence of a stronger gradient below the tropopause, which should be low for a well-mixed troposphere. b) Difference between the normalised gradient at the tropopause as shown in Fig. 7 and the gradient 0.5 km below as shown in panel (a). Here, higher values indicate a stronger differentiation between the cross-tropopause value and the well-mixed troposphere. All values have been normalised to the seasonal O_3 mixing ratio at the respective tropopause.

https://doi.org/10.5194/egusphere-2025-1589
Preprint. Discussion started: 24 April 2025

Appendix D: Mean tropopause height

Table D1. Mean height of the tropopause for the CARIBIC data set where geopotential height information is available. All values are given in kilometres [km].

Tropopause definition	Mean	Spring	Summer	Autumn	Winter
Chemical_{O_3}	10.00	9.69	10.19	10.16	9.98
$\text{Dynamic}_{1.5}$	9.83	9.27	10.47	10.05	9.37
$\text{Dynamic}_{2.0}$	10.21	9.65	10.84	10.42	9.77
$\text{Dynamic}_{3.5}$	10.86	10.28	11.45	11.09	10.46
Thermal	10.97	10.28	11.72	11.23	10.47

https://doi.org/10.5194/egusphere-2025-1589
Preprint. Discussion started: 24 April 2025

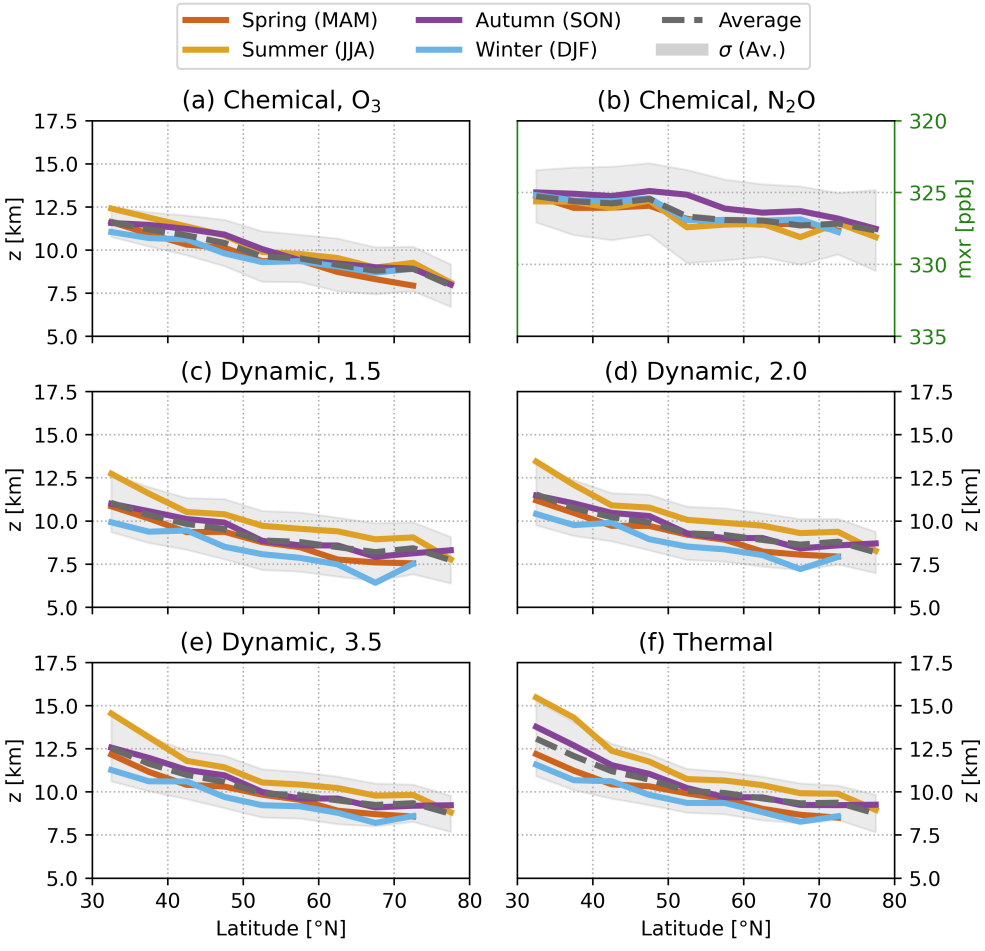

Figure D1. Latitude-binned (5°) mean seasonal tropopause height across the whole CARIBIC measurement period. Panels (a) and (b)–(f) are given in geopotential height, while in panel (b) the mean seasonal value of the statistically evaluated baseline of the chemical$_{N_2O}$ tropopause is given. The grey shading indicates the standard deviation of the seasonal average.

https://doi.org/10.5194/egusphere-2025-1589
Preprint. Discussion started: 24 April 2025

References

Assonov, S., Brenninkmeijer, C., Schuck, T., and Umezawa, T.: N2O as a Tracer of Mixing Stratospheric and Tropospheric Air Based on CARIBIC Data with Applications for CO2, Atmospheric Environment, 79, 769–779, https://doi.org/10.1016/j.atmosenv.2013.07.035, 2013.

Bethan, S., Vaughan, G., and Reid, S. J.: A Comparison of Ozone and Thermal Tropopause Heights and the Impact of Tropopause Definition on Quantifying the Ozone Content of the Troposphere, Quarterly Journal of the Royal Meteorological Society, 122, 929–944, https://doi.org/10.1002/qj.49712253207, 1996.

Bisht, J. S. H., Machida, T., Chandra, N., Tsuboi, K., Patra, P. K., Umezawa, T., Niwa, Y., Sawa, Y., Morimoto, S., Nakazawa, T., Saitoh, N., and Takigawa, M.: Seasonal Variations of SF6, CO2, CH4, and N2O in the UT/LS Region Due to Emissions, Transport, and Chemistry, Journal of Geophysical Research: Atmospheres, 126, https://doi.org/10.1029/2020JD033541, 2021.

Brenninkmeijer, C. A. M., Crutzen, P., Boumard, F., Dauer, T., Dix, B., Ebinghaus, R., Filippi, D., Fischer, H., Franke, H., Frieß, U., Heintzenberg, J., Helleis, F., Hermann, M., Kock, H. H., Koeppel, C., Lelieveld, J., Leuenberger, M., Martinsson, B. G., Miemczyk, S., Moret, H. P., Nguyen, H. N., Nyfeler, P., Oram, D., Penkett, S., Platt, U., Pupek, M., Ramonet, M., Randa, B., Reichelt, M., Rhee, T. S., Rohwer, J., Rosenfeld, K., Scharffe, D., Schlager, H., Schumann, U., Slemr, F., Sprung, D., Stock, P., Thaler, R., Valentino, F., Van Velthoven, P., Waibel, A., Wandel, A., Waschitschek, K., Wiedensohler, A., Xueref-Remy, I., Zahn, A., Zech, U., and Ziereis, H.: Civil Aircraft for the Regular Investigation of the Atmosphere Based on an Instrumented Container: The New CARIBIC System, Atmospheric Chemistry and Physics, 7, 4953–4976, https://doi.org/10.5194/acp-7-4953-2007, 2007.

Fischer, H., Wienhold, F. G., Hoor, P., Bujok, O., Schiller, C., Siegmund, P., Ambaum, M., Scheeren, H. A., and Lelieveld, J.: Tracer Correlations in the Northern High Latitude Lowermost Stratosphere: Influence of Cross-Tropopause Mass Exchange, Geophysical Research Letters, 27, 97–100, https://doi.org/10.1029/1999GL010879, 2000.

Gettelman, A., Hoor, P., Pan, L. L., Randel, W. J., Hegglin, M. I., and Birner, T.: The Extratropical Upper Troposphere and Lower Stratosphere, Reviews of Geophysics, 49, https://doi.org/10.1029/2011RG000355, 2011.

HALO: Mission PHILEAS (Probe High Latitude Export of Air from the Asian Summer Monsoon), https://doi.org/10.17616/R39Q0T, 2025.

Hersbach, H., Bell, B., Berrisford, P., Hirahara, S., Horányi, A., Muñoz-Sabater, J., Nicolas, J., Peubey, C., Radu, R., Schepers, D., Simmons, A., Soci, C., Abdalla, S., Abellan, X., Balsamo, G., Bechtold, P., Biavati, G., Bidlot, J., Bonavita, M., De Chiara, G., Dahlgren, P., Dee, D., Diamantakis, M., Dragani, R., Flemming, J., Forbes, R., Fuentes, M., Geer, A., Haimberger, L., Healy, S., Hogan, R. J., Hólm, E., Janisková, M., Keeley, S., Laloyaux, P., Lopez, P., Lupu, C., Radnoti, G., de Rosnay, P., Rozum, I., Vamborg, F., Villaume, S., and Thépaut, J.-N.: The ERA5 Global Reanalysis, Quarterly Journal of the Royal Meteorological Society, 146, 1999–2049, https://doi.org/10.1002/qj.3803, 2020.

Hoerling, M. P., Schaack, T. K., and Lenzen, A. J.: Global Objective Tropopause Analysis, Monthly Weather Review, 119, 1816–1831, https://doi.org/10.1175/1520-0493(1991)119<1816:GOTA>2.0.CO;2, 1991.

Kunz, A., Konopka, P., Müller, R., and Pan, L. L.: Dynamical Tropopause Based on Isentropic Potential Vorticity Gradients, Journal of Geophysical Research, 116, D01 110, https://doi.org/10.1029/2010JD014343, 2011.

Millán, L. F., Hoor, P., Hegglin, M. I., Manney, G. L., Boenisch, H., Jeffery, P., Kunkel, D., Petropavlovskikh, I., Ye, H., Leblanc, T., and Walker, K.: Exploring Ozone Variability in the Upper Troposphere and Lower Stratosphere Using Dynamical Coordinates, Atmospheric Chemistry and Physics, 24, 7927–7959, https://doi.org/10.5194/acp-24-7927-2024, 2024.

https://doi.org/10.5194/egusphere-2025-1589
Preprint. Discussion started: 24 April 2025

Müller, S.: Untersuchung von Mischungs- und Transportprozessen in der oberen Troposphäre - unteren Stratosphäre basierend auf in-situ Spurengasmessungen, Ph.D. thesis, Johannes Gutenberg-Universität Mainz, Mainz, 2015.

Obersteiner, F.: FAIROmeta, https://doi.org/10.5281/zenodo.11275355, 2024.

Pan, L. L., Kunz, A., Homeyer, C. R., Munchak, L. A., Kinnison, D. E., and Tilmes, S.: Commentary on Using Equivalent Latitude in the Upper Troposphere and Lower Stratosphere, Atmospheric Chemistry and Physics, 12, 9187–9199, https://doi.org/10.5194/acp-12-9187-2012, 2012.

Petzold, A., Thouret, V., Gerbig, C., Zahn, A., Brenninkmeijer, C. A., Gallagher, M., Hermann, M., Pontaud, M., Ziereis, H., Boulanger, D., Marshall, J., NéDélec, P., Smit, H. G., Friess, U., Flaud, J. M., Wahner, A., Cammas, J. P., Volz-Thomas, A., Thomas, K., Rohs, S., Bundke, U., Neis, P., Berkes, F., Houben, N., Berg, M., Tappertzhofen, M., Blomel, T., Pätz, W., Filges, A., Boschetti, F., Verma, S., Baum, S., Athier, G., Cousin, J. M., Sauvage, B., Blot, R., Clark, H., Gaudel, A., Gressent, A., Auby, A., Fontaine, A., Gautron, B., Bennouna, Y., Petetin, H., Karcher, F., Abonnel, C., Dandin, P., Beswick, K., Wang, K. Y., Rauthe-Schöch, A., Baker, A. K., Riede, H., Gromov, S., Zimmermann, P., Thorenz, U., Scharffe, D., Koeppel, C., Slemr, F., Schuck, T. J., Umezawa, T., Ditas, J., Cheng, Y., Schneider, J., Williams, J., Neumaier, M., Christner, E., Fischbeck, G., Safadi, L., Petrelli, A., Gehrlein, T., Heger, S., Dyroff, C., Weber, S., Assmann, D., Rubach, F., Weigelt, A., Stratmann, G., Stock, P., Penth, L., Walter, D., Heue, K. P., Allouche, Y., Marizy, C., Hermira, J., Bringtown, S., Saueressig, G., Seidel, N., Huf, M., Waibel, A., Franke, H., Klaus, C., Stosius, R., Baumgardner, D., Braathen, G., Paulin, M., and Garnett, N.: Global-Scale Atmosphere Monitoring by in-Service Aircraft - Current Achievements and Future Prospects of the European Research Infrastructure IAGOS, Tellus, Series B: Chemical and Physical Meteorology, 6, 1–24, https://doi.org/10.3402/tellusb.v67.28452, 2015.

Prather, M. J., Zhu, X., Tang, Q., Hsu, J., and Neu, J. L.: An Atmospheric Chemist in Search of the Tropopause, Journal of Geophysical Research: Atmospheres, 116, https://doi.org/10.1029/2010JD014939, 2011.

Reed, R. J.: A Study of a Characteristic Tpye of Upper-Level Frontogenesis, Journal of Meteorology, 12, 226–237, https://doi.org/10.1175/1520-0469(1955)012<0226:ASOACT>2.0.CO;2, 1955.

Riese, M., Hoor, P., Rolf, C., and Kunkel, D.: Quasi-Horizontal Transport of Asian Summer Monsoon Air during the PHILEAS Campaign in Summer and Autumn 2023, Tech. Rep. EGU24-6647, Copernicus Meetings, https://doi.org/10.5194/egusphere-egu24-6647, 2024.

Schuck, T. and Obersteiner, F.: IAGOS-CARIBIC Whole Air Sampler Data (V2024.01.12), https://doi.org/10.5281/zenodo.10495039, 2024.

Schuck, T. J., Brenninkmeijer, C. A. M., Slemr, F., Xueref-Remy, I., and Zahn, A.: Greenhouse Gas Analysis of Air Samples Collected Onboard the CARIBIC Passenger Aircraft, Atmospheric Measurement Techniques, 2, 449–464, https://doi.org/10.5194/amt-2-449-2009, 2009.

Schuck, T. J., Ishijima, K., Patra, P. K., Baker, A. K., MacHida, T., Matsueda, H., Sawa, Y., Umezawa, T., Brenninkmeijer, C. A., and Lelieveld, J.: Distribution of Methane in the Tropical Upper Troposphere Measured by CARIBIC and CONTRAIL Aircraft, Journal of Geophysical Research Atmospheres, 117, https://doi.org/10.1029/2012JD018199, 2012.

Schuck, T. J., Lefrancois, F., Gallmann, F., Wang, D., Jesswein, M., Hoker, J., Bönisch, H., and Engel, A.: Establishing Long-Term Measurements of Halocarbons at Taunus Observatory, Atmospheric Chemistry and Physics, 18, 16 553–16 569, https://doi.org/10.5194/acp-18-16553-2018, 2018.

SPARC: SPARC Report on the Lifetimes of Stratospheric Ozone-Depleting Substances, Their Replacements, and Related Specie, SPARC Report 6, SPARC, 2013.

https://doi.org/10.5194/egusphere-2025-1589
Preprint. Discussion started: 24 April 2025

Sprung, D. and Zahn, A.: Acetone in the Upper Troposphere/Lowermost Stratosphere Measured by the CARIBIC Passenger Aircraft: Distribution, Seasonal Cycle, and Variability, Journal of Geophysical Research: Atmospheres, 115, https://doi.org/10.1029/2009JD012099, 2010.

Tinney, E. N., Homeyer, C. R., Elizalde, L., Hurst, D. F., Thompson, A. M., and Stauffer, R. M.: A Modern Approach to a Stability-Based Definition of the Tropopause, MONTHLY WEATHER REVIEW, 150, https://doi.org/10.1175/MWR-D-22-0174.1, 2022.

Turhal, K., Plöger, F., Clemens, J., Birner, T., Weyland, F., Konopka, P., and Hoor, P.: Variability and Trends in the Potential Vorticity (PV)-Gradient Dynamical Tropopause, Atmospheric Chemistry and Physics, 24, 13 653–13 679, https://doi.org/10.5194/acp-24-13653-2024, 2024.

Umezawa, T., Baker, A. K., Oram, D., Sauvage, C., O'Sullivan, D., Rauthe-Schöch, A., Montzka, S. A., Zahn, A., and Brenninkmeijer, C. A. M.: Methyl Chloride in the Upper Troposphere Observed by the CARIBIC Passenger Aircraft Observatory: Large-scale Distributions and Asian Summer Monsoon Outflow, Journal of Geophysical Research: Atmospheres, 119, 5542–5558, https://doi.org/10.1002/2013JD021396, 2014.

Wilcox, L. J., Hoskins, B. J., and Shine, K. P.: A Global Blended Tropopause Based on ERA Data. Part I: Climatology, Quarterly Journal of the Royal Meteorological Society, 138, 561–575, https://doi.org/10.1002/qj.951, 2012.

WMO: Definition of the Tropopause, WMO Bulletin, 6, 136, 1957.

WMO: Atmospheric Ozone 1985. Assessment of Our Understanding of the Processes Controlling Its Present Distribution and Change, Tech. Rep. 16, World Meteorological Organisation, Geneva, Switzerland, 1986.

Zahn, A., Weppner, J., Widmann, H., Schlote-Holubek, K., Burger, B., Kühner, T., and Franke, H.: A Fast and Precise Chemiluminescence Ozone Detector for Eddy Flux and Airborne Application, Atmospheric Measurement Techniques, 5, 363–375, https://doi.org/10.5194/amt-5-363-2012, 2012.

Zahn, A., Obersteiner, F., Gehrlein, T., Neumaier, M., Dyroff, C., Förster, E., Sprung, D., Van Velthoven, P., Xueref-Remy, I., Ziereis, H., Bundke, U., Gerbig, C., Scharffe, D., Slemr, F., Weber, S., Hermann, M., Cheng, Y., and Bönisch, H.: IAGOS-CARIBIC MS Files Collection (V2024.10.28), https://doi.org/10.5281/zenodo.14000090, 2024.